

Performance of the G_0W_0 Method in Predicting the Electronic Gap of TiO_2 Nanoparticles

Ángel Morales-García, Rosendo Valero, Francesc Illas*

Departament de Ciència de Materials i Química Física & Institut de Química Teòrica i Computacional (IQTUB), Universitat de Barcelona, c/ Martí i Franqués 1, 08028 Barcelona, Spain

Abstract

Using a relativistic all-electron description and numerical atomic centered orbital basis set the performance of the G_0W_0 method on the electronic band gap of $(\text{TiO}_2)_n$ nanoparticles ($n=1-20$) is investigated. Results are presented for G_0W_0 on top of hybrid (PBE0 and a modified version with 12.5% of Fock exchange) functionals. The underestimation of the electronic band gap from Kohn-Sham orbital energies is corrected by the quasiparticle energies from G_0W_0 method which are consistent with the variational ΔSCF approach. A clear correlation between both methods exists regardless of the hybrid functional employed. In addition, the vertical ionization potential and electron affinity from quasiparticle energies show a systematic correlation with the ΔSCF calculated values. On the other hand, the shape of the nanoparticles promotes some deviations on the electronic band gap. In conclusion, this study shows (i) a systematic correlation exists between band gaps, ionization potentials and electron affinities of TiO_2 nanoparticles as predicted from variational ΔSCF and G_0W_0 methods, (ii) that the G_0W_0 approach can be successfully used to study the electronic band gap of realistic size nanoparticles at an affordable computational cost with a ΔSCF accuracy giving results that are directly related with those from photoemission spectroscopy, (iii) the quasiparticle energies are explicitly required to shed light on the photocatalytic properties of TiO_2 and (iv) that G_0W_0 approach emerges as an accurate method to investigate the photocatalytic properties of both nanoparticles and extended semiconductor.

Introduction

Nanoparticles and nanoclusters have been widely investigated due to the broad variety of applications in biomedical, optical and electronic fields.^{1,2} In general, nanoparticles show remarkably high catalytic performance compared with the bulk phase due to their large surface area and quantum confinement effect.³ Particularly, semiconductor nanoparticles display specific electronic properties such as the lowest excitation —often referred to as band gap as in the corresponding bulk material— that make them especially attractive for applications in photocatalysis.⁴ For instance, to use sunlight for photocatalytic water splitting, leading to an almost inexhaustible sustainable energy source, requires materials with band gaps in the UV-VIS range.

Not surprisingly, the size and morphology of the nanoparticles are important factors in determining their electronic structure and, hence, their potential photocatalytic activity.⁵ Experimentally it is difficult to discern between the effect of size and shape on the electronic properties of nanoparticles. On the other hand, computational modeling provides an unbiased approach to analyze the influence of these factors on the electronic properties. Using appropriate models, it is possible to represent different morphologies for a given composition or to vary the composition for a given morphology. The effect of shape and size of nanoparticle in defining the corresponding band gap and concomitant photoactivity has been illustrated in recent work on bottom-up^{6,7} and top-down⁸ models of TiO₂ nanoparticles including explicitly over one thousand atoms. In these works, the band gap of the nanoparticles has been studied using density functional theory (DFT) methods. In particular, the electronic (or fundamental, E_{gap}) and the optical (O_{gap}) band gap⁹ have been considered. The former can be measured from photoemission techniques whereas the latter is accessible through optical spectroscopy. The charged states either of cationic (free extra hole, h^+) or anionic (free extra electron, e^-) nanoparticles are associated to E_{gap} whereas the generation of an excited electron–hole (e^-h^+) pair corresponds to O_{gap} (more details can be found in Ref. [6] and references therein). Note that, in absence of excitons, O_{gap} and E_{gap} of a bulk solid coincide. Precisely, the difference between these two quantities, usually referred to as the exciton binding energy (ΔE_{ex}), has been used to measure the bulk like character of TiO₂ nanoparticles of different size.⁶⁻⁸

In the framework of DFT, the use of the Kohn-Sham (KS) one-electron energies to approach either E_{gap} or O_{gap} is a common practice, even although values predicted from Generalized Gradient Approximation (GGA) exchange correlation potentials are too small,¹⁰ even incorrectly describing antiferromagnetic insulators such as NiO as metals.^{11,12} In the case of nanoparticles, the band gap is calculated as the difference between the highest occupied molecular orbital (HOMO) and the lowest

unoccupied molecular orbital (LUMO) KS energies ($\Delta E_{\text{H-L}}$) and it is also strongly underestimated (up to 50%) at the standard GGA level. The use of hybrid approaches leads to values closer to experiment¹³ although the amount of Fock exchange or the choice of the parameters defining more sophisticated range-separated hybrid functionals appear to constitute serious issues.^{14,15} In fact, a 12.5% of Fock exchange has been found to reproduce the band gap of anatase and rutile polymorphs of TiO₂ whereas a 25%, as in PBE0, nicely reproduces the experimental gap in ZnO bulk structure.¹⁶ Recently, Perdew *et al.*¹⁷ provided a theoretical basis to the well-known empiric fact that hybrid functionals as PBE0 yield realistic generalized KS gaps for semiconductor materials. In the case of the E_{gap} , a more reliable method which is directly applicable to nanoparticles, is to use a ΔSCF approach which implies taking differences of total energy of a given N electron system and that of the system with $N+1$ or $N-1$ electronic system. This difference is the total energy upon adding (or removing) an electron, and is therefore the electron affinity (or ionization energy). However, this approach is not directly applicable to extended solids since it results in charged unit cells requiring some to introduce some charge compensation technique.

An alternative to ΔSCF methods to calculate the E_{gap} is provided by the many-body perturbation theory GW approach suggested long ago by Hedin¹⁸ and only applicable in practice thanks to the availability of more powerful computational and methodological developments.¹⁹ The GW acronym stems from the way the self-energy is calculated, as it is given by the product of the Green function G and the screened Coulomb interaction W . GW allows one to calculate the quasiparticle (qp) energies and their values correspond directly to electron removal or addition energies, being ideally matching those calculated using ΔSCF method and requiring the calculation of the N electron system only. The simplest level of GW is the so-called G_0W_0 approximation.²⁰⁻²² It yields reasonably accurate qp energies and band gap in good agreement with the experiments for extended systems, while an assessment of G_0W_0 for finite systems is emerging.²³⁻²⁷ In general, the evaluation of the qp energies often leads to a good correlation with experimental values for the energies of the valence excitation and gaps in several semiconductors^{21,28-31} and also in molecules.³²

To explore the accuracy of G_0W_0 method in describing E_{gap} of oxide nanoparticles we focus on titanium dioxide (TiO₂), a material broadly studied due to its diverse technological applications; in particular in photocatalysis.³³⁻³⁷ The present study is in the line of previous work using the G_0W_0 approach to interpret photoelectron spectroscopy experiments involving (TiO₂)_n clusters with up to 10 units,³⁸ to explore two crystalline phases of dye-sensitized TiO₂ clusters,³⁹ and to study the properties of rutile TiO₂ nanoclusters.⁴⁰ In the present work, TiO₂ nanoparticles containing up to 20 units are chosen as models to investigate the trends in E_{gap} as predicted using $\Delta E_{\text{H-L}}$ from KS orbital energies, ΔSCF and G_0W_0 methods. Using a relativistic, all-electron, description with numerical

atomic centered orbital basis set and modified hybrid functional, we show that a systematic correlation exists between band gaps, ionization potentials and electron affinities of TiO₂ nanoparticles as predicted from Δ SCF and G_0W_0 methods, which could open the way for an accurate description of the electronic properties of oxide nanoparticles of realistic size at an affordable computational cost.

Models and Computational Details

All calculations are performed using the first-principles electronic structure theory based on DFT explicitly including all electrons. A numerical atom-centered (NAO) orbital basis set is used, as implemented in the Fritz Haber Institute *ab initio* molecular simulations (FHI-aims) program package.⁴¹ A light grid and tier-1 basis set is used, which has a quality similar to a valence triple- ζ plus polarization Gaussian Type Orbitals (GTO) basis.⁸ Additionally, light grid and tier-2 basis set is also used to better assess the accuracy of tier-1 basis set (see Supporting Information). The convergence threshold for geometrical relaxation of all nanoparticles is set to 10^{-4} eV \AA^{-1} . The presence of a transition element like Ti requires the inclusion of relativistic effects to ensure a correct convergence during the relaxation steps, zero atomic order regular approximation (ZORA)^{42,43} is hence used in the calculations. Different hybrid functionals including a fraction of non-local Fock exchange are employed. These are PBE0 (25% Fock) and a modification of PBE0 containing 12.5% Fock and hereafter referred to as PBEx.⁴⁴ The reason for using PBEx is that it has been proven to properly reproduce the main features of the electronic structure of stoichiometric and reduced anatase and rutile.³⁹ Moreover, in view of the strong dependence of the G_0W_0 method with respect to the initial density,⁴⁵ hybrid functionals should provide a better starting point.⁴⁶

A set of (TiO₂)_n nanoparticles with n running from 1 to 20 units (Figure 1) is selected from the recent works^{6,47,48} with the structures determined by global optimization using interatomic potentials⁶ and, in each case, refined at the PBE, PBEx and PBE0 level using the NAO basis set commented above. The electronic band gap of the (TiO₂)_n particles has been estimated from different approaches but using always the minimum energy structure (Figure 1) consistent with the exchange-correlation potential used. The first one consists simply in taking the difference between the HOMO and LUMO orbital energies and will be denoted as ΔE_{H-L} . The second method consist in making use of total energy differences and involves the vertical ionization potential (IP_v) and vertical electron affinity (EA_v): $E_{\text{gap}} = \text{IP}_v - \text{EA}_v$. This approach is usually referred to as Δ SCF, as it requires the variational self-consistent energy of the neutral, cation and anion. For a given DFT method, the Δ SCF approach provides the best possible results, as it implies variational energies. The third approach explored and benchmarked with respect to the Δ SCF results is the G_0W_0

approach. This makes use of a perturbative expansion to include the many-body effects through the many-body self-energy Σ . In the GW approximation⁴⁹ the self-energy is calculated as:

$$\Sigma^{GW}(r, r', \omega) = \frac{i}{2\pi} \int d\omega' G(r, r', \omega') W(r, r', \omega' + \omega) \quad (1)$$

where $G(r, r', \omega')$ is the one-particle Green's function and $W(r, r', \omega)$ is the screened Coulomb interaction. The GW self-energy can be used to perturbatively correct the KS eigenvalues by means of the linearized quasiparticle equation:

$$\epsilon_i^{qp} = \epsilon_i^{KS} - \langle \psi_i^{KS} | \hat{V}_{xc}^{KS} - \hat{\Sigma}^{GW}(\epsilon_i^{qp}) | \psi_i^{KS} \rangle \quad (2).$$

In the G_0W_0 or one-shot GW , the self-energy is calculated only once, whereas a more rigorous approach would require a fully self-consistent evaluation of Σ . Since the ϵ_i^{qp} quasiparticle (qp) energies in Eq. (2) are evaluated perturbatively on top of a preliminary single-particle calculation, the G_0W_0 approach strongly depends on the starting point;^{19,40,41} an issue that has been studied in detail in recent articles⁵⁰ with the general conclusions that hybrid functional provide better results. In the following we refer to G_0W_0 based on PBE_x and PBE0 as $G_0W_0@PBE_x$ and $G_0W_0@PBE0$, respectively. For a detailed account of the all-electron implementation of GW in FHI-aims we refer the interested reader to the original article of Ren *et al.*⁵¹ It must be mentioned that performing GW calculations in an all-electron code such as FHI-aims has the advantage that possible pseudopotential errors are avoided, and eventually it can be used in periodic systems where the use of the variational Δ SCF approach requires additional approximations. As discussed extensively in the literature, the pseudopotential derived errors do not affect ground-state DFT energy but may become significant in GW calculations if there is significant spatial overlap between core and valence wave-functions.⁵² This issue was recently solved by Maggio *et al.*⁵³ reporting a careful comparison of GW qp energies obtained using Gaussian type orbitals and plane waves. In addition, the compact and inherently local nature of the NAO basis functions leads to a more rapid convergence with the number of basis functions.⁵⁴

Results and Discussion

We first focus on the trend of the E_{gap} as a function of the number of TiO_2 units as predicted by the $\Delta E_{\text{H-L}}$, Δ SCF and G_0W_0 approaches. The vertical ionization potentials and electron affinities obtained from Δ SCF and G_0W_0 methods are also discussed and compared with other theoretical and experimental works. Finally, the effect of the nanoparticle shape will be also investigated for the

case of larger TiO₂ nanoparticles, in this work containing 18 to 20 units. It must be noted that light grid and tier-2 basis set is used to evaluate the basis set convergence at $G_0W_0@PBE0$ level in (TiO₂)_n nanoparticles with n= 1-11 units, obtaining similar results than those obtained using light grid and tier-1 basis set (further details are given in Supporting Information).

Electronic band gap.

Figure 2 shows the E_{gap} calculated following G_0W_0 , ΔSCF and $\Delta E_{\text{H-L}}$ procedures and using the PBE_x and PBE0 hybrid functionals. Overall, the trends are systematically consistent for each method, with values from PBE0 being larger than those obtained from PBE_x, although the effect is quite large for $\Delta E_{\text{H-L}}$ (Figure 2c) and much less for G_0W_0 and ΔSCF , already indicating the higher accuracy of the latter approaches. More in detail, relative to G_0W_0 and ΔSCF , E_{gap} associated to $\Delta E_{\text{H-L}}$ is systematically underestimated and particularly sensitive to the exact exchange energy contribution associated to the hybrid functional (see Figure 2c). The percent of exact exchange energy contribution induces a significant increase of the band gap according to $E_{\text{gap}}(\text{PBE0})/E_{\text{gap}}(\text{PBE}_x) \approx 0.6$ ratio. Note that, for a given functional, much larger particles are required to reach the bulk value depending on the method of calculation of the DFT energy.⁸ The ΔSCF method is more reliable and, actually, for a given DFT method provides the best possible estimate since all energy values used to estimate ionization potential and the electron affinity are variationally obtained — i.e. from separate well-converged self-consistent calculations. Therefore, for either PBE0 or PBE_x, the ΔSCF values are taken as the **appropriate approach for the DFT level.**

Let us now focus on the performance of the many body perturbation theory (MBPT) based on G_0W_0 method. Here, the E_{gap} values are fully consistent with those arising from ΔSCF calculation to the point that a systematic correlation between both methods exist (see Figure 3a). **This result opens the possibility to use G_0W_0 for larger systems like extended solids where the variational ΔSCF is not suitable. G_0W_0 approach emerges as the appropriate computational technique to describe the electronic properties of semiconductors.** This is consistent with previous works using GW techniques to approach the properties of bulk TiO₂.⁵⁵ In the case of bulk TiO₂, however, in Ref. 49 the accuracy of G_0W_0 was established by comparing to the experimental value only whereas here the comparison between G_0W_0 and ΔSCF for a significant number of cases provides a more solid basis. This is further evidenced by the linear fit shown in Figure 3. It is noted that the oscillations observed in the smallest nanoparticles (n= 1–3) are related to the nanoparticle structure; similar oscillations have been previously reported.⁴² Although the E_{gap} goes down, it is far from bulk values (see Figure 2). This is not surprising, since TiO₂ nanoparticles of ~20 nm diameter composed by more than 10000 units are required to reach the bulk behavior.⁸

Comparing the electronic band gaps obtained by G_0W_0 to those obtained from Δ SCF and ΔE_{H-L} leads again to systematic correlation, as displayed in Figure 3. The straight line is particularly noted for the case of $E_{\text{gap}}(G_0W_0)$ versus $E_{\text{gap}}(\Delta\text{SCF})$ in Figure 3a, where the E_{gap} values calculated at PBE α and PBE0 levels are grouped in the same fitting, showing that the functional (exact exchange energy contribution) affects equally in both methods. As it has been discussed above, the effect of the functional is much more pronounced when E_{gap} is calculated via ΔE_{H-L} . This is the reason why two different linear fittings are observed in Figure 3b. Although the functional promotes the shifts in the straight line, the deviation between both approaches is systematically consistent for PBE α and PBE0, as evidenced by fitting parameters in Figure 3. Similar linear correlations have been previously reported for a wide range of materials.^{56,57}

Up to here, the present analysis provides compelling evidence that the **electronic band gap calculated using G_0W_0 is consistent with the Δ SCF approach**, thus overcoming the problems arising from the use of Kohn-Sham orbital energies which are largely affected by self-interaction errors. Nevertheless, one can argue that the success is due to an error cancellation consequence of a systematic error in the calculation of vertical ionization potentials and electron affinities. Results in the next subsection show that this is not the case.

Vertical Ionization potential and electron affinity.

In MBPT it is shown that the energy of the GW eigenvalues, usually referred to as quasiparticles (qp) energies, corresponds directly to electron removal or addition energies.^{19,58} Therefore, vertical ionization potential (IP_v) and electron affinity (EA_v) can be obtained directly from the qp energies as $IP_v = -qp_{\text{HOMO}}$ and $EA_v = -qp_{\text{LUMO}}$, respectively. Table 1 compiles the IP_v and EA_v values for the set of explored TiO_2 nanoparticles as obtained from G_0W_0 and Δ SCF methods. For comparison, the corresponding potentials for periodic TiO_2 determined through combined experimental-theoretical approaches^{59,60} are included. Regarding the experimental values for $(\text{TiO}_2)_n$ nanoparticles, photoemission data are only available for negatively charged clusters⁶¹ and, therefore, we are not able to directly compare with the results for neutral clusters. However, our results are compared to computational analyses reported previously by Chiodo *et al.*⁶² for small $(\text{TiO}_2)_n$ nanoparticles with $n = 3-10$ using all-electron calculations with relativistic effects in consistency with our results. These authors reported ranges of 7.8–9.5 eV and 2.5–3.2 eV for IP_v and EA_v , respectively. Our results reported in Table 1 are fully consistent with those reported by Chiodo *et al.*⁵⁶ Additionally, EA_v for clusters from 3 to 10 units were experimentally determined to be in the range 2.6–3.5 eV.⁵⁵

To further analyze the trends in IP_v and EA_v values as predicted from Δ SCF and G_0W_0 calculations, Figure 4 presents a linear correlation between the two sets of calculated IP_v and EA_v values. The amount of exact exchange energy contribution in the PBE0 and PBEEx hybrid functional affects the results in the same way which is consistent with results in Figure 3a. In general, G_0W_0 predicts IP_v and EA_v values systematically slightly below those calculated using Δ SCF (see Table 1). To end this subsection, note that the values of IP_v/EA_v are significantly higher/lower than the corresponding potentials for periodic TiO_2 anatase as it was already reported.⁵⁴ These differences are due to the quantum confinement effect in the TiO_2 nanoparticles.

Influence of the shape of TiO_2 Nanoparticles on band gap.

For a given $(TiO_2)_n$ nanoparticle size, distinct isomers exist within a narrow range of energy per unit.⁶ Figure S1 shows the set of isomers investigated and the electronic band gap (ΔE_{H-L} , Δ SCF and G_0W_0) are reported in Tables S3 and S4 at PBEEx and PBE0 level, respectively. It is therefore interesting to analyze the performance of the G_0W_0 approach on determining the E_{gap} of the different isomers. With this idea in mind, the electronic properties of two different isomers, obtained during the global optimization search,⁶ are investigated for the three largest particles considered in the present work which are those with $n = 18, 19$ and 20 (Figure 5). For a given size (n), the energy differences for the different isomers are almost the same for the PBEEx and PBE0 methods; the $n=19$ nanoparticle shows the largest energy difference followed by nanoparticles with $n=20$ and $n=18$. The energy differences may seem large but correspond to ~ 0.2 eV/unit only.

The results reported in Table 2 clearly show the influence of the nanoparticle shape, in agreement with previous findings reported by Cho *et al.*⁶ The present results show that the minimum energy structures with a different atomic structure show smaller band gaps than the most stable ones, with differences in E_{gap} as large as 1 eV. It is worth pointing out that these observations are consistent with experiments reported by Ba-Abbad *et al.*⁶³ Depending on the shape and size of the synthesized nanoparticles, these authors observed E_{gap} variations of 0.15 eV. Nevertheless, even if the shape has a marked influence in small nanoparticles, this is notably reduced when increasing the size of the particles. Therefore, small band gap deviations in large nanoparticles composed by hundreds of TiO_2 units are expected independently of the shape. Finally, note that the difference between $E_{gap}(\Delta$ SCF) and $E_{gap}(G_0W_0)$ for the higher energy isomers is similar to that corresponding to the global minima, as expected, indicating the performance of the G_0W_0 method in predicting E_{gap} of TiO_2 nanoparticles barely depends on the particle size.

Conclusions

The E_{gap} of $(\text{TiO}_2)_n$ ($n=1-20$) nanoparticles is assessed employing $\Delta E_{\text{H-L}}$ from KS orbital energies, ΔSCF and G_0W_0 methods by means of a relativistic all-electron description with numerical atomic centered orbital basis sets and using PBE x (12.5% Fock) and PBE0 (25% Fock) hybrid functionals. The systematic, well-known, underestimation predicted by $\Delta E_{\text{H-L}}$ is largely corrected by the G_0W_0 method, which leads to results in good agreement with those obtained for the variational ΔSCF approach. The present analysis clearly proves that a systematic correlation exists between G_0W_0 and ΔSCF independently of the hybrid functional employed. This correlation is not fortuitous, arising for instance from error cancellation, since a similar correlation is obtained for the vertical ionization potential and electron affinity. The differences of $\Delta E_{\text{H-L}}$ in TiO_2 isomers corresponding to the largest nanoparticles show variations within the experimental range. In a similar way, using the G_0W_0 approach small deviations are expected for nanoparticles composed by hundreds of atoms.

It has been shown that a systematic correlation between electronic band gap, ionization potential and electron affinity of TiO_2 nanoparticles exists between the variational ΔSCF and G_0W_0 methods. Therefore, G_0W_0 calculations provide one a successfully way to investigate the electronic band gap of realistic size of TiO_2 nanoparticles (~ 20 nm diameter) at an affordable computational cost using FHI-AIMS code with a ΔSCF precision. One of the main advantage of G_0W_0 method is that the quasiparticles energies are compared directly with results from photoemission spectroscopy. This information is of great interest to understand and improve the photocatalytic activity of TiO_2 nanoparticles in processes as CO_2 photoreduction and water splitting by light. This study opens the possibility for using G_0W_0 in larger systems like extended semiconductors where the the variational ΔSCF is not suitable.

Acknowledgements

This research was supported by the Spanish MINECO/FEDER CTQ2015-64618-R grant and, in part, by Generalitat de Catalunya (grants 2014SGR97 and XRQTC) and by the NOMAD Center of Excellence project, which received funding from the European Union's Horizon 2020 research and innovation programme under grant agreement No 676580. A. M. G. thanks to Spanish *Ministerio de Economía y Competitividad* for the *Juan de la Cierva* postdoctoral grant (FJCI-2015-23760) and FI acknowledges additional support from the 2015 ICREA Academia Award for Excellence in University Research. Computational time at the Marenstrum supercomputer has been provided by the Barcelona Supercomputing Centre through grants from Red Española de Supercomputación and

the COMPHOTOCAT project 2014112608 of the Partnership for Advanced Computing in Europe (PRACE).

Associated Content

The Supporting Information is available free of charge on the ACS Publications website at DOI:

XXXXXXXXXXXX

Tables S1 and S2 compile all electronic band gaps, vertical ionization potentials and vertical electron affinities at the PBE_x and PBE0 levels, respectively. Figure S1 shows the isomers for 10, 13, 14, 15, 16, 17, 18, 19 and 20 units and Tables S3 and S4 compile the electronic band gaps, vertical ionization potentials and vertical electron affinities for the isomers of Figure S1 at the PBE_x and PBE0 levels, respectively. Table S5 compiles the electronic band gaps, vertical ionization potentials and vertical electron affinities at G_0W_0 @PBE0 using tier-2 basis set.

Author Information

Corresponding Author e-mail: francesc.illas@ub.edu

Table 1.- Range of IP_v and EA_v using ΔSCF and G_0W_0 methods at PBE x and PBE0 level. Potentials for periodic TiO_2 anatase are also included.^{53,54} All values are in eV.

	ΔSCF	G_0W_0
PBEx		
IP_v	9.30 – 10.14	9.10 – 9.78
EA_v	2.49 – 3.94	1.70 – 3.06
PBE0		
IP_v	9.84 – 10.59	9.54 – 10.16
EA_v	2.39 – 3.42	1.63 – 2.53
Periodic TiO_2 anatase		
IP_v	7.82 – 8.30	
EA_v	4.67 – 5.10	

Table 2.- Electronic band gap of the global minima and one higher energy isomer of the $(\text{TiO}_2)_n$ nanoparticles with $n=18-20$ as predicted from $\Delta E_{\text{H-L}}$, ΔSCF and G_0W_0 calculations carried out with the PBE_x and PBE0 hybrid functionals. Numbers correspond to the most stable structures located at the top in Figure 5. Those located between parenthesis correspond to the bottom structures in Figure 5. ΔE has the same meaning as in the caption of Figure 5. All values are in eV.

n	ΔE	$\Delta E_{\text{H-L}}$	ΔSCF	G_0W_0
PBE_x				
18	0(2.09)	4.01 (3.48)	6.07 (5.60)	7.38 (6.62)
19	0 (3.68)	4.22 (3.23)	6.28 (5.55)	7.06 (6.32)
20	0 (2.34)	4.66 (3.46)	6.58 (5.55)	7.49 (6.58)
PBE0				
18	0 (1.96)	5.34 (4.75)	6.93 (6.37)	7.93 (7.07)
19	0 (3.71)	5.47 (4.49)	7.02 (6.25)	7.46 (6.78)
20	0 (2.65)	5.94 (4.77)	7.55 (6.30)	7.92 (7.07)

Figure 1. Structure of global minima of the $(\text{TiO}_2)_n$ nanoparticles, $n = 1-20$ used in this work. Blue and red spheres correspond to titanium and oxygen atoms, respectively.

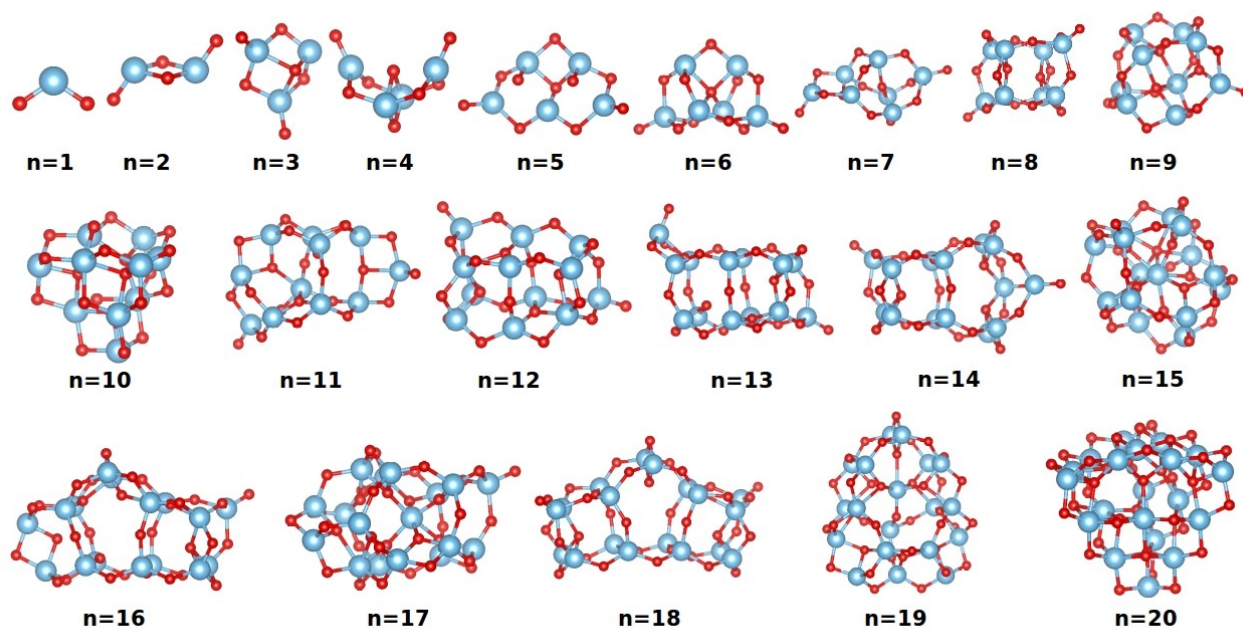


Figure 2. Calculated electronic band gap of $(\text{TiO}_2)_n$ nanoparticles using (a) G_0W_0 , (b) ΔSCF and (c) $\Delta E_{\text{H-L}}$ methods at PBE \times (orange) and PBE0 (purple) levels. The dashed lines in (c) correspond to the experimental band gap of bulk anatase (3.2 eV) and rutile (3.03 eV) systems which are provided for comparison. All these values are compiled in Figures S1 and S2 at PBE \times and PBE0, respectively.

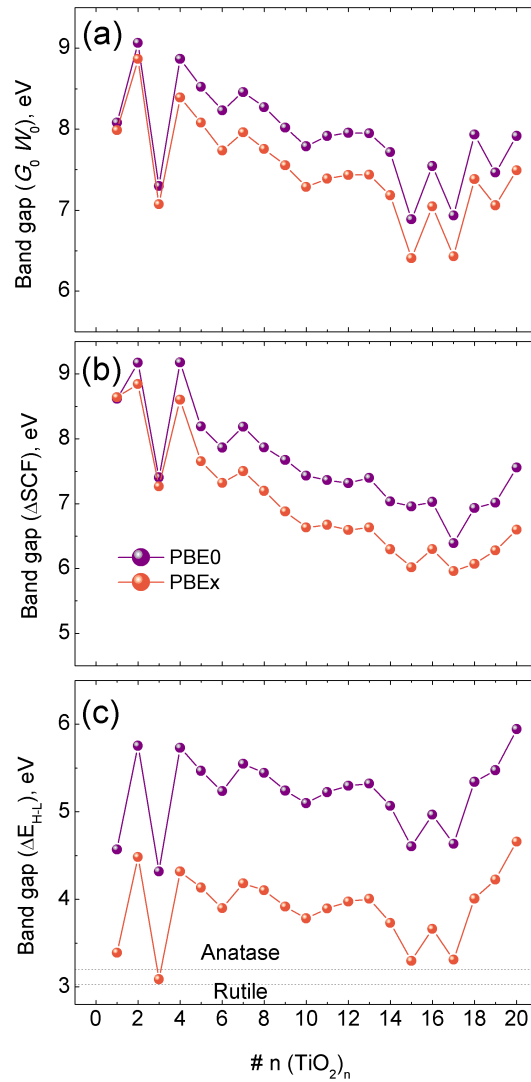


Figure 3. Linear relationship between $E_{\text{gap}}(G_0W_0)$ and (a) $E_{\text{gap}}(\Delta\text{SCF})$ and (b) $E_{\text{gap}}(\Delta E_{\text{H-L}})$. The smallest nanoparticles, $n=1, 2$ and 3 units are not considered in the linear fitting due to their oscillation effects. Fitting equations are shown in the inset. For simplicity, the E_{gap} term is removed from the axis legends and linear regressions. All these values are compiled in Figures S1 and S2 at PBE α and PBE0, respectively.

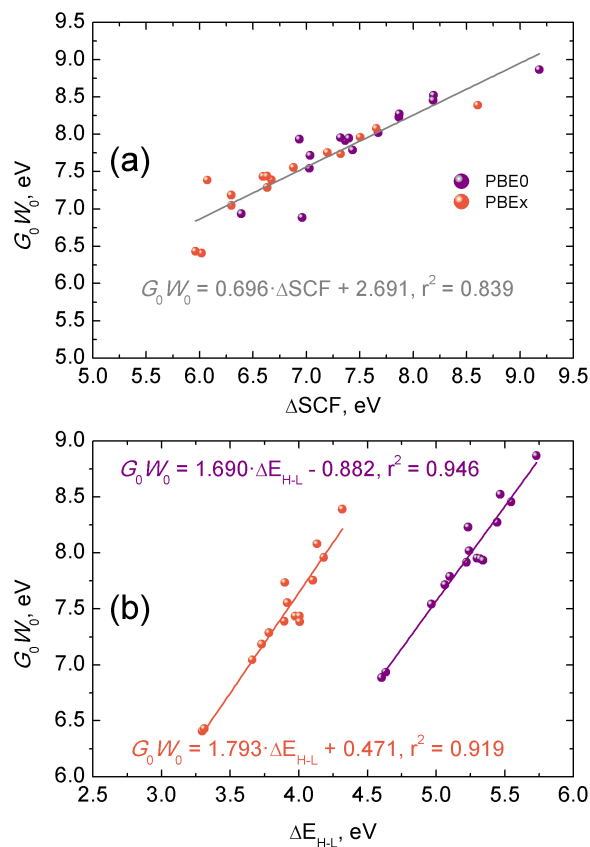


Figure 4.- Linear relationship between (a) vertical ionization potential (IP_v) and (b) vertical electron affinity (EA_v) obtained from G_0W_0 and Δ SCF calculations. Results for the smallest nanoparticles, $n=1, 2$ and 3 units are not considered in the linear fitting due to their oscillation effects. The linear regression is also displayed. All these values are compiled in Figures S1 and S2 at PBEx and PBE0, respectively.

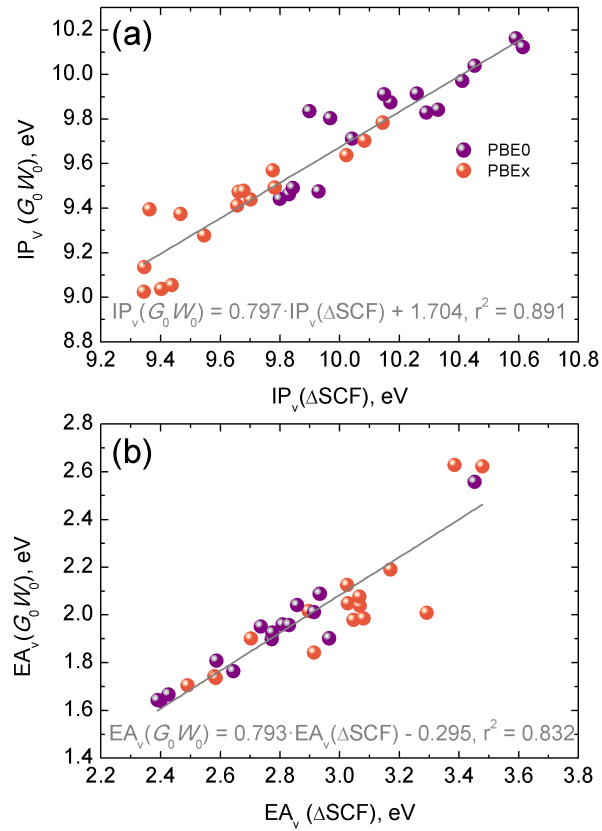
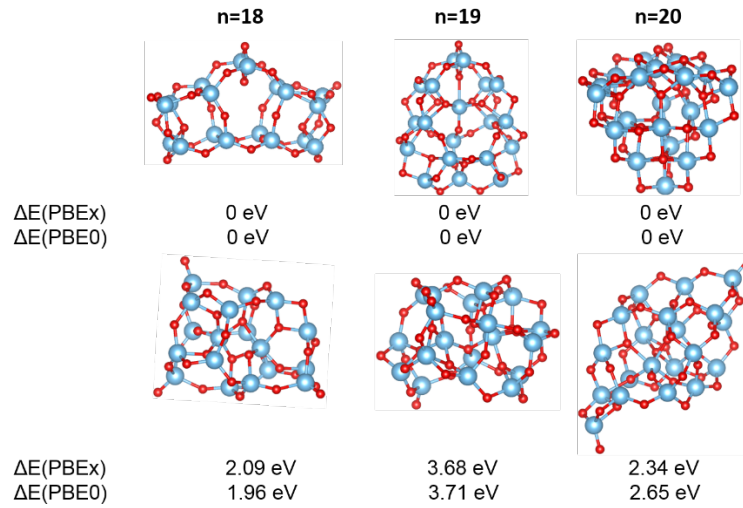


Figure 5.- $(\text{TiO}_2)_n$ nanoparticles with $n = 18, 19$ and 20 units. The nanoparticles shown at the top are the most stable energetically and they are compared with the nanoparticles below, which have different shape and higher energies. Positive values of ΔE are associated with energies above the global minima, which are taken as reference.



References

- ¹ Stark, W. J.; Stoessel, P. R.; Wohlleben, W.; Hafner, A. Industrial applications of nanoparticles. *Chem. Soc. Rev.* **2015**, *44*, 5793-5805.
- ² Kittelson, D. B. Engines and nanoparticles: a review. *J. Aerosol Sci.* **1998**, *29*, 575-588.
- ³ Sang, L.; Zhao, Y.; Burda, C. TiO₂ Nanoparticles as Functional Buildings Blocks. *Chem. Rev.* **2014**, *114*, 9283-9318.
- ⁴ Beydoun, D.; Amal, R.; Low, G.; McEvoy, S. Role of Nanoparticles in Photocatalysis. *J. Nanopar. Res.* **1999**, *1*, 439-458.
- ⁵ Chen, X.; Mao, S. S. Titanium Dioxide Nanomaterials: Synthesis, Properties, Modifications and Applications. *Chem. Rev.* **2007**, *107*, 2891-2959.
- ⁶ Lamiel Garcia, O.; Cuko, A.; Calatayud, M.; Illas, F.; Bromley, S. T. Predicting Size-Dependent Emergence of Crystallinity in Nanomaterials: Titania Nanoclusters Versus Nanocrystals. *Nanoscale*, **2017**, *9*, 1049-1058.
- ⁷ Cho, D.; Ko, K. C.; Lamiel-García, O.; Bromley, S. T.; Lee, J. Y.; Illas, F.; Effect of Size and Structure on the Ground-State and Excited-State Electronic Structure of TiO₂ Nanoparticles. *J. Chem. Theory. Comput.* **2016**, *12*, 3751-3763.
- ⁸ Lamiel-García, O.; Ko, K. C.; Lee, J. Y.; Bromley, S. T.; Illas, F.; When anatase nanoparticles become bulk-like: Properties of realistic TiO₂ nanoparticles in the 1-6 nm size range from all electron relativistic density functional theory based calculations. *J. Chem. Theory. Comput.* **2017**, *13*, 1785-1793.
- ⁹ Bredas, J. L.; Mind the gap! *Mater. Horiz.* **2014**, *1*, 17-19.
- ¹⁰ Bagayoko, D.; Understanding density functional theory (DFT) and completing it in practice. *AIP Adv.* **2014**, *7*, 127104 (1-12).
- ¹¹ Terakura, K.; Oguchi, T.; Williams, A. R.; Klüber, J. Band theory of insulating transition-metal monoxides: Band-structure calculations. *Phys. Rev. B* **1984**, *30*, 4734-4747.
- ¹² Shen, Z.-X.; List, R. S.; Dessau, D. S.; Wells, B. O.; Jepsen, O.; Arko, A. J.; Bartlett, R.; Shih, C. K.; Parmigiani, F.; Huang, J. C.; Lindberg, P. A. P. Electronic structure of NiO: Correlation and band effects. *Phys. Rev. B* **1991**, *44*, 3604-3626.
- ¹³ Muscat, J.; Wander, A.; Harrison, N. M. On the prediction of band gaps from hybrid functional theory. *Chem. Phys. Lett.*, **2001**, *342*, 397-401.
- ¹⁴ Di Valentin, C.; Pacchioni, G. Spectroscopic Properties of Doped and Defective Semiconducting Oxides from Hybrid Density Functional Calculations. *Acc. Chem. Res.*, **2014**, *47*, 3233-3241.

-
- ¹⁵ Viñes, F.; Lamiel-García, O.; Ko, K. C.; Lee, Y. J.; Illas, F. Systematic study of the effect of HSE functional internal parameters on the electronic structure and band gap of a representative set of metal oxides. *J. Comput. Chem.* **2017**, *38*, 781-789.
- ¹⁶ Viñes, F.; Illas, F. Electronic structure of stoichiometric and reduced ZnO from periodic relativistic all electron hybrid density functional calculations using numeric atom-centered orbitals. *J. Comput. Chem.* **2017**, *38*, 523-529.
- ¹⁷ Perdew, J. P.; Yang, W.; Burke, K.; Yang, Z.; Gross, E. K. U.; Scheffler, M.; Scuseria, G. E.; Henderson, T. M.; Zhang, I. Y.; Ruzinsky, A.; Peng, H.; Sun, J.; Trushin, E.; Görling, A. Understanding band gaps of solids in generalized Kohn-Sham theory. *Proc. Natl. Acad. Sci.* **2017**, *114*, 2801-2806.
- ¹⁸ Hedin, L. New Method for Calculating the One-Particle Green's Function with Application to the Electron-Gas Problem. *Phys. Rev.* **1965**, *139*, A796-A823.
- ¹⁹ Aryasetiawan, F.; Gunnarsson, O. The *GW* method. *Rep. Prog. Phys.* **1998**, *61*, 237-312.
- ²⁰ van Schilfhaarde, M.; Kotani, T.; Faleev, S. Quasiparticle Self-Consistent *GW* Theory. *Phys. Rev. Lett.* **2006**, *96*, 226402 (1-4).
- ²¹ Shishkin, M.; Kresse, G. Self-consistent *GW* calculations for semiconductors and insulators. *Phys. Rev. B* **2007**, *75*, 235102 (1-9).
- ²² Fuchs, F.; Furthmüller, J.; Bechstedt, F. Quasiparticle band structure based on a generalized Kohn-Sham scheme. *Phys. Rev. B* **2007**, *76*, 115109 (1-8).
- ²³ Qian, X.; Umari, P.; Marzari, N. Photoelectron properties of DNA and RNA bases from many-body perturbation theory. *Phys. Rev. B* **2011**, *84*, 075103 (1-8).
- ²⁴ Sharifzadeh, S.; Biller, A.; Kronik, L.; Neaton, J. B. Quasiparticle and optical spectroscopy of the organic semiconductors pentacene and PTCDA from first-principles. *Phys. Rev. B* **2012**, *85*, 125307 (1-11).
- ²⁵ Bruneval, F. Ionization energy of atoms obtained from *GW* self-energy or from random phase approximation total energies. *J. Chem. Phys.* **2012**, *136*, 194107 (1-10).
- ²⁶ Ma, Y.; Rohlfing, M.; Molteni, C. Modeling the Excited States of Biological Chromophores within Many-Body Green's Function Theory. *J. Chem. Theory Comput.* **2010**, *6*, 257-265.
- ²⁷ Faber, C.; Attaccalite, C.; Olevano, V.; Runge, E.; Blasé, X. First-principles *GW* calculations for DNA and RNA nucleobases. *Phys. Rev. B* **2011**, *83*, 115123.
- ²⁸ Faleev, S. M.; van Schilfhaarde, M.; Kotani, T. All-Electron Self-Consistent *GW* Approximation: Application to Si, MnO, and NiO. *Phys. Rev. Lett.* **2004**, *93*, 126406 (1-4).
- ²⁹ Rödl, C.; Fuchs, F.; Furthmüller, J.; Bechstedt, F. Quasiparticle band structures of the

-
- antiferromagnetic transition-metal oxides MnO, FeO, CoO, and NiO. *Phys. Rev. B* **2009**, *79*, 235114 (1-8).
- ³⁰ Jiang, H.; Gomez-Abal, R. I.; Rinke, P.; Scheffler, M. First-principles modelling of localized *d* states with the *GW@LDA+U* approach. *Phys. Rev. B* **2010**, *82*, 045108 (1-16).
- ³¹ Kang, W.; Hybertsen, M. S. Quasiparticle and optical properties of rutile and anatase TiO₂. *Phys. Rev. B* **2010**, *82*, 085203 (1-11).
- ³² van Setten, M. J.; Caruso, F.; Sharifzadeh, S.; Ren, X.; Scheffler, M.; Liu, F.; Lischner, J.; Lin, L.; Delippe, J. R.; Louie, S. G.; Yang, C.; Weigend, F.; Neaton, J. B.; Evers, F.; Rinke, P. *GW100*: Benchmarking *G₀W₀* for Molecular Systems. *J. Chem. Theory Comput.* **2015**, *11*, 5665-5687.
- ³³ Anne, M.; Dulay, M. T. Heterogeneous photocatalysis. *Chem. Rev.* **1993**, *93*, 341-357.
- ³⁴ Xu, H.; Ouyang, S.; Liu, L.; Reunchan, P.; Umezawa, N. Ye, J. Recent advances in TiO₂-based photocatalysis. *J. Mater. Chem. A* **2014**, *2*, 12642-12661.
- ³⁵ Hashimoto, K.; Irie, H.; Fujishima, A. TiO₂ Photocatalysis: A Historical Overview and Future Prospects. *Jpn. J. Apply. Phys.* **2005**, *44*, 8269-8285.
- ³⁶ Fujishima, A.; Xintong, Z.; Tryk, D. A. TiO₂ photocatalysis and related surface phenomena. *Surf. Sci. Rep.* **2008**, *63*, 515-582.
- ³⁷ Chen, X.; Shen, S.; Guo, L.; Mao, S. S. Semiconductor-based Photocatalytic Hydrogen Generation. *Chem. Rev.* **2010**, *110*, 6503-6570.
- ³⁸ Marom, N.; Kim, M.; Chelikowsky, J. R. Structure Selection Based on High Vertical Electron Affinity for TiO₂ Clusters. *Phys. Rev. Lett.* **2012**, *108*, 106801.
- ³⁹ Marom, N.; Moussa, J. E.; Ren, X.; Tkatchenko, A.; Chelikowsky J. R. Electronic structure of dye-sensitized TiO₂ clusters from many-body perturbation theory. *Phys. Rev. B* **2011**, *84*, 245115
- ⁴⁰ Hung, L.; Baishya, K.; Ögut, S. First-principles real-space study of electronic and optical excitations in rutile TiO₂ nanocrystals. *Phys. Rev. B* **2014**, *90*, 165424.
- ⁴¹ Blum, V.; Gehrke, R.; Hanke, F.; Havu, P.; Ren, X.; Reuter, K.; Scheffler, M. *Ab initio* molecular simulations with numeric atom-centered orbitals. *Comput. Phys. Commun.* **2009**, *180*, 2175-2196.
- ⁴² Chang, Ch.; Pelissier, M.; Durand, Ph. Regular Two-Component Pauli-Like Effective Hamiltonians in Dirac Theory. *Phys. Scr.* **1986**, *34*, 394.
- ⁴³ van Lenthe, E.; Baerends, E. J.; Snijders, J. G. Relativistic regular two-component Hamiltonians. *J. Chem. Phys.* **1993**, *99*, 4597.
- ⁴⁴ Ko, K. C.; Lamiel-García, O.; Lee, J. Y.; Illas, F. Performance of a modified hybrid functional

-
- in the simultaneous description of stoichiometric and reduced TiO₂ polymorphs. *Phys. Chem. Chem. Phys.* **2016**, *18*, 12357-12367.
- ⁴⁵ Liao, P.; Carter, E. A. Testing variations of the *GW* approximation on strongly correlated transition metal oxides: hematite (α -Fe₂O₃) as a benchmark. *Phys. Chem. Chem. Phys.* **2011**, *13*, 15189-15199
- ⁴⁶ Ren, X.; Rinke, P.; Scheffler, M. Exploring the Random Phase Approximation: Application to CO adsorbed on Cu (111). *Phys. Rev. B* **2009**, *80*, 045402.
- ⁴⁷ Berardo, E.; Hu, H. S.; Shevlin, S. A.; Woodley, S. M.; Kowalski, K.; Zwijnenburg, M. A. Modeling Excited States in TiO₂ Nanoparticles: On the Accuracy of a TD-DFT Based Description. *J. Chem. Theory Comput.* **2014**, *10*, 1189-1199.
- ⁴⁸ Berardo, E.; Hu, H. S.; van Dam, H. J.; Shevlin, S. A.; Woodley, S. M.; Kowalski, K.; Zwijnenburg, M. A. Describing excited state relaxation and localization in TiO₂ nanoparticles using TD-DFT. *J. Chem. Theory Comput.* **2014**, *10*, 5538-5548.
- ⁴⁹ Bagus, P. S.; Self-Consistent π -Field Wave Functions for Holes States of Some Ne-Like and Ar-Like Ions. *Phys. Rev.* **1965**, *139*, A619.
- ⁵⁰ Govoni, M.; Galli, G. Large Scale GW Calculations. *J. Chem. Theory Comput.* **2015**, *11*, 2680-2696.
- ⁵¹ Ren, X.; Rinke, P.; Blum, V.; Wieferink, J.; Tkatchenko, A.; Sanfilippo, A.; Reuter, K.; Scheffler, M. Resolution-of-identity approach to Hartree-Fock, hybrid density functionals, RPA, MP2 and *GW* with numeric atom-centered orbital basis functions. *New J. Phys.* **2012**, *14*, 053020 (55 pp)
- ⁵² Ku, W.; Eguiluz, A. G. Band-Gap Problem in Semiconductors Revisited: Effects of Core States and Many-Body Self-Consistency. *Phys. Rev. Lett.* **2002**, *12*, 126401 (1-4).
- ⁵³ Maggio, E.; Liu, P.; van Setten, Michiel J.; Kresse, G. *GW*100: A Plane Wave perspective for Small Molecules. *J. Chem. Theory Comput.* **2017**, *13*, 635-648.
- ⁵⁴ Samsonidze, G.; Jain, M.; Deslippe, J.; Cohen, Marvin L.; Louie, S. G. Simple Approximation Physical Orbitals for *GW* Quasiparticle Calculations. *Phys. Rev. Lett.* **2011**, *107*, 186404 (1-5).
- ⁵⁵ Gerosa, M.; Bottani, C. E.; Caramella, L.; Onida, G.; Di Valentin, C.; Pacchioni, G. Electronic Structure and Phase Stability of Oxide Semiconductors: Performance of Dielectric-Dependent Hybrid Functional DFT, Benchmarked Against *GW* Band Structure Calculations and Experiments. *Phys. Rev. B*, 2015, **91**, 155201.
- ⁵⁶ Shishkin, M.; Kresse, G. Self-consistent *GW* calculations for semiconductors and insulators. *Phys. Rev. B* **2007**, *75*, 235102.

-
- ⁵⁷ Demiroglu, I.; Tosoni, S.; Illas, F.; Bromley Stefan T. Bandgap engineering through nanoporosity. *Nanoscale* **2014**, *6*, 1181-1187.
- ⁵⁸ Marom, N.; Ren, X.; Moussa, J. E.; Chelikowsky, J. R.; Kronik, L.; Electronic structure of copper phthalocyanine from G_0W_0 calculations. *Phys. Rev. B* **2011**, *84*, 195143 1-8.
- ⁵⁹ Buckeridge, J.; Butler, K. T.; Catlow, C. R. A; Logsdail, A. J.; Scanlon, D. O.; Shevlin, S. A.; Woodley, S. M.; Sokol, A. A.; Walsh, A. Polymorph Engineering of TiO₂: Demonstrating How Absolute Reference Potentials are Determined by Local Coordination. *Chem. Mater.* **2015**, *27*, 3844-3851.
- ⁶⁰ Scanlon, D. O.; Dunnill, C. W.; Buckeridge, J.; Shevlin, S. A.; Logsdail, A. J.; Woodley, S. M.; Catlow, C. R. A.; Powell, M. J.; Palgrave, R. G.; Parkin, I. P.; Watson, G. K.; Keal, T. W.; Sherwood, P.; Walsh, A.; Sokol, A. A. Band Alignment of Rutile and Anatase TiO₂. *Nat. Mater.* **2013**, *12*, 798-801.
- ⁶¹ Zhai, H. J.; Wang, L. S.; Probing the Electronic Structure and Band Gap Evolution of Titanium Oxide Clusters (TiO₂)_n⁻ ($n = 1-10$) Using Photoelectron Spectroscopy. *J. Am. Chem. Soc.* **2007**, *129*, 3022-3026.
- ⁶² Chiodo, L.; Salazar, M.; Romero, A. H.; Laricchia, S.; Della Sala, F.; Rubio, A. Structure, electronic, and optical properties of TiO₂ atomic clusters: An ab initio study. *J. Chem. Phys.* **2011**, *135*, 244704 1-10.
- ⁶³ Ba-Abbad, M.; Kadhum, A. A. H.; Mohamad, A., B.; Takriff, M. S.; Sopian, K.; Synthesis and Catalytic Activity of TiO₂ Nanoparticles for Photochemical Oxidation of Concentrated Chlorophenols under Direct Solar Radiation. *Int. J. Electrochem. Sci.* **2012**, *7*, 4871-4888.

TOC Graphic

